

Organization of Subunits in the Membrane Domain of the Bovine F-ATPase Revealed by Covalent Cross-linking*

Received for publication, February 23, 2015, and in revised form, March 24, 2015. Published, JBC Papers in Press, April 7, 2015, DOI 10.1074/jbc.M115.645283

Jennifer Lee^{†1}, ShuJing Ding[‡], Thomas B. Walpole^{†1}, Andrew N. Holding[§], Martin G. Montgomery[‡], Ian M. Fearnley[‡], and John E. Walker^{‡2}

From the [†]The Medical Research Council Mitochondrial Biology Unit, Cambridge Biomedical Campus, Hills Road, Cambridge CB2 0XY, United Kingdom and [§]The Medical Research Council Laboratory of Molecular Biology, Cambridge Biomedical Campus, Francis Crick Avenue, Cambridge CB2 0QH, United Kingdom

Background: Bovine mitochondrial F-ATPase has six uncharacterized membrane subunits.

Results: Labeled lysines have been mapped onto its incomplete structure.

Conclusion: Subunit ATP8 extends about 70 Å from the membrane into the peripheral stalk. The N-terminal regions of five others are in the mitochondrial matrix.

Significance: Subunit ATP8 is in the stator. Five other subunits form a subdomain.

The F-ATPase in bovine mitochondria is a membrane-bound complex of about 30 subunits of 18 different kinds. Currently, ~85% of its structure is known. The enzyme has a membrane extrinsic catalytic domain, and a membrane intrinsic domain where the turning of the enzyme's rotor is generated from the transmembrane proton-motive force. The domains are linked by central and peripheral stalks. The central stalk and a hydrophobic ring of c-subunits in the membrane domain constitute the enzyme's rotor. The external surface of the catalytic domain and membrane subunit a are linked by the peripheral stalk, holding them static relative to the rotor. The membrane domain contains six additional subunits named ATP8, e, f, g, DAPIT (diabetes-associated protein in insulin-sensitive tissues), and 6.8PL (6.8-kDa proteolipid), each with a single predicted transmembrane α -helix, but their orientation and topography are unknown. Mutations in ATP8 uncouple the enzyme and interfere with its assembly, but its roles and the roles of the other five subunits are largely unknown. We have reacted accessible amino groups in the enzyme with bifunctional cross-linking agents and identified the linked residues. Cross-links involving the supernumerary subunits, where the structures are not known, show that the C terminus of ATP8 extends ~70 Å from the membrane into the peripheral stalk and that the N termini of the other supernumerary subunits are on the same side of the membrane, probably in the mitochondrial matrix. These experiments contribute significantly toward building up a complete structural picture of the F-ATPase.

The F-ATPase from bovine mitochondria is a membrane-bound protein assembly of ~30 polypeptides of 18 different kinds with a combined molecular mass of ~650 kDa (1, 2). The enzyme has a membrane extrinsic globular F_1 -catalytic domain that is attached to the membrane domain by central and

peripheral stalks. The F_1 domain is an assembly of three α -subunits and three β -subunits arranged in alternation in a spherical complex around an elongated α -helical structure in the γ -subunit (3), and the three catalytic sites of the enzyme lie at interfaces between the α - and β -subunits. The γ -subunit extends from the $\alpha_3\beta_3$ -spherical structure to the membrane domain, where it is augmented by the δ - and ϵ -subunits in the contact region or "foot" with the membrane domain. Together, the γ -, δ -, and ϵ -subunits constitute the central stalk, and the foot makes extensive contacts with a hydrophobic ring of eight c-subunits in the membrane domain of the enzyme (4). The c₈-ring and the central stalk constitute the rotor of the enzyme. Their rotation as an ensemble at ~100 Hz carries energy into the catalytic sites of the enzyme, and the turning of the rotor brings about conformational changes in the three catalytic sites in the F_1 domain that lead to the binding of substrates and the formation of ATP and its release into the matrix. The region of contact between the rotating c-ring and subunit a, another membrane protein of unknown structure, provides the transmembrane pathway for protons to pass from the intermembrane space into the mitochondrial matrix (5), allowing energy from the transmembrane proton-motive force generated by respiration to drive the turning of the rotor. Subunit a forms part of the stator and is in contact with the membrane domain of subunit b, which extends through the peripheral stalk, an elongated subcomplex of single copies of subunits b, d, F_6 , and oscp (6–9) to the "top" of the $\alpha_3\beta_3$ domain (10). Thus, the stator consists of the $\alpha_3\beta_3$ domain, plus subunits oscp, b, d, F_6 , and a, and it remains static relative to the turning of the rotor. Atomic resolution structures have been established for the F_1 c-ring (4) and peripheral stalk domains (7, 8), and a mosaic structure of the enzyme has been built within the envelope of a low resolution structure of the entire complex determined by electron cryo-microscopy (11).

Also associated with the membrane domain of the bovine enzyme are six small proteins, ATP8, e, f, g, DAPIT³ (diabetes

* This work was supported by the intramural program of the Medical Research Council (MRC Grant U105663150 (to J. E. W.)).

⌘ Author's Choice—Final version free via Creative Commons CC-BY license.

¹ Recipients of Medical Research Council graduate studentships.

² To whom correspondence should be addressed. E-mail: walker@mrc-mbu.cam.ac.uk.

³ The abbreviations used are: DAPIT, diabetes-associated protein in insulin-sensitive tissues; 6.8PL, 6.8 kDa proteolipid; DSS, disuccinimidyl suberate;

associated protein in insulin sensitive tissues), and 6.8 kDa proteolipid (6.8PL), with molecular masses in the range 6.3–11.4 kDa (1, 2, 12–14). Each has a single predicted transmembrane α -helix, and based largely on their staining intensities in gel analyses of the subunit composition of the enzyme, it is assumed that there is one copy of each protein per F-ATPase complex, but there are no definitive quantitative data to support this assumption. These proteins are usually referred to as the “supernumerary” subunits as there are no orthologs in bacterial F-ATPases, and they appear not to be involved directly in the synthesis of ATP. In the yeast enzyme the orthologs of subunits e and g are associated with the formation of dimers of the F-ATPase (15, 16), and they probably play the same role in the mammalian enzyme.

In this study the identification of covalent cross-links introduced into the subunits of the bovine F-ATPase by reaction of exposed amino groups with isotopically labeled bifunctional reagents has been employed as a means of gaining information about the orientation and location of the supernumerary subunits within the bovine enzyme complex.

Experimental Procedures

Analytical Methods—Protein concentrations were estimated by the bicinchoninic acid assay (17). Protein compositions were analyzed by SDS-PAGE in 12–22% or 4–20% polyacrylamide gradient gels or by blue native PAGE (18, 19). Proteins were detected by staining with Coomassie Blue dye.

Purification of Monomeric Bovine F-ATPase—Phosphate-washed bovine mitochondrial membranes (10 mg/ml) were extracted with buffer containing 1% (w/v) *n*-dodecyl- β -D-maltoside and 20 mM Tris·HCl, pH 7.3, 10% glycerol (v/v), 0.15 M sodium chloride, 20 mM EDTA, 1 mM tris(2-carboxyethyl)phosphine, 1-palmitoyl-2-oleoyl-*sn*-glycerophosphocholine (100 μ g/ml), 1-palmitoyl-2-oleoyl-*sn*-glycerophosphoethanolamine (33 μ g/ml), and 1-palmitoyl-2-oleoyl-*sn*-glycero-phospho-(1'-rac-glycerol) (33 μ g/ml). The ATP hydrolytic activity of the F-ATPase, measured by an enzyme-coupled assay (20), was inhibited with a recombinant protein consisting of residues 1–60 of the natural bovine inhibitor protein, IF₁, with a C-terminal glutathione *S*-transferase domain plus hexahistidine, and the active enzyme complex was purified as described before (21) except that the detergent in the buffers, *n*-dodecyl- β -D-maltoside, was replaced by 0.05% (w/v) *n*-dodecyl- β -D-maltose-neopentyl glycol. The ATP hydrolytic activity of the purified enzyme was 50–90 μ mol of ATP hydrolyzed/min/mg, and the sensitivity of this activity to inhibition by 0.01% (w/v) oligomycin was 95–99%, indicating that the enzyme was almost entirely coupled in its F₀ domain. Purified F-ATPase was dialyzed against buffer consisting of 20 mM HEPES, pH 7.3, 0.05% *n*-dodecyl- β -D-maltose-neopentyl glycol (w/v), 10% glycerol (v/v), 50 mM sodium chloride, 1 mM tris(2-carboxyethyl)phosphine, 2 mM magnesium sulfate, 2 mM ATP, 1-palmitoyl-2-oleoyl-*sn*-glycero-phosphocholine (100 μ g/ml), 1-palmitoyl-2-oleoyl-*sn*-glycerophosphoethanolamine (33 μ g/ml), 1-palmitoyl-2-oleoyl-*sn*-glycerophospho-(1'-rac-glycerol) (33 μ g/ml).

Chemical Cross-linking—Four deuterium-labeled cross-linking agents were employed. Disuccinimidyl suberate (DSS) and disuccinimidyl glutarate (DSG) are membrane-permeable, whereas di(sulfosuccinimidyl) glutarate (DSSG) and bi(sulfosuccinimidyl) suberate (BS³) are membrane impermeable. In the isotope-labeled versions, DSS(*d*₀/*d*₁₂), BS³(*d*₀/*d*₁₂), DSG(*d*₀/*d*₆), and DSSG(*d*₀/*d*₆), (Creative Molecules), the numbers of deuterium atoms, *d*, in the two acyl arms of each reagent are indicated by the subscripted numerals and were supplied and used at molar ratios of the two isotopic forms of 1:1 (22, 23). Freshly purified bovine F-ATPase was diluted to a concentration of 1.22 mg/ml in buffer consisting of 20 mM HEPES, pH 7.3, 0.05% *n*-dodecyl- β -D-maltose-neopentyl glycol (w/v), 10% glycerol (v/v), 50 mM sodium chloride, 1 mM tris(2-carboxyethyl)phosphine, 2 mM magnesium sulfate, 2 mM ATP, 1-palmitoyl-2-oleoyl-*sn*-glycero-phosphocholine (100 μ g/ml), 1-palmitoyl-2-oleoyl-*sn*-glycerophosphoethanolamine (33 μ g/ml), and 1-palmitoyl-2-oleoyl-*sn*-glycero-phospho-(1'-rac-glycerol) (33 μ g/ml). The reaction conditions were optimized with DSS(*d*₀/*d*₁₂) dissolved in dimethyl sulfoxide added at concentrations of 0.1–5 mM. The reactions were carried out at pH values of 6.8, 7.3, and 8.0 for 2, 4, or 20 h and at temperatures of 20 or 37 °C. The optimal cross-linking conditions were 2 μ M F-ATPase (1.16 mg/ml) at pH 8.0 reacted with 2 mM DSS(*d*₀/*d*₁₂) for 2 h at 20 °C. BS³(*d*₀/*d*₁₂), DSG(*d*₀/*d*₆) and DSSG(*d*₀/*d*₆) were reacted with the enzyme at the same concentration and under the same conditions. The reactions were terminated by the addition of ammonium bicarbonate to a final concentration of 200 mM. The solutions were kept at 20 °C for 30 min. Insoluble material was removed by centrifugation (10,000 \times g, 5 min, 20 °C), and the supernatants were analyzed by SDS-PAGE and blue native-PAGE. The cross-linked F-ATPases were precipitated with ethanol for 18 h at –20 °C, and the precipitates were recovered by centrifugation and redissolved in 6 M guanidinium hydrochloride in 20 mM Tris-HCl buffer. The proteins were reduced with tris(2-carboxyethyl)phosphine, alkylated with iodoacetamide (10 mM), and re-precipitated. These samples of *S*-alkylated cross-linked F-ATPases were analyzed in three different ways. First, the precipitates were dissolved in 100 mM ammonium bicarbonate and digested at 37 °C for 16 h with trypsin (trypsin:protein, 1:100, w:w). Portions of the digests were diluted with 0.1% formic acid for mass spectrometric analysis. Second, other samples of *S*-alkylated and cross-linked F-ATPase were fractionated by SDS-PAGE, and gel bands or gel regions were excised and digested with trypsin (24). Third, an *S*-alkylated sample of F-ATPase cross-linked with DSS(*d*₀/*d*₁₂) was dialyzed for 18 h against 100 mM ammonium bicarbonate and digested at 37 °C with trypsin (F-ATPase: trypsin, 100:1, w:w). The digest was dried and fractionated on a column of PolySULFOethyl A (50 mm long \times 1.0 mm inner diameter; 300 Å pore size; PolyLC, Columbia, MD) equilibrated at a flow rate of 50 μ l/min in 10 mM potassium phosphate buffer, pH 2.7, containing 10% acetonitrile. Peptides were eluted with a gradient of 0–1 M potassium chloride in 20 mM potassium phosphate, pH 3.0, containing 10% acetonitrile (see Fig. 1). Fractions were dried and dissolved in 0.3% trifluoroacetic acid, and salts were removed from the samples by passage through a reverse-phase C₁₈ ZipTip (Millipore).

DSG, disuccinimidyl glutarate; DSSG, di(sulfosuccinimidyl) glutarate; BS³, bi(sulfosuccinimidyl) suberate.

Membrane Subunits of Bovine F-ATPase

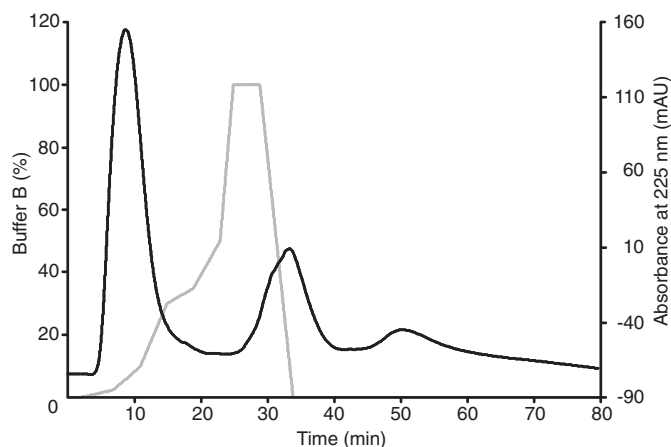


FIGURE 1. **Fractionation of a tryptic digest of bovine F-ATPase cross-linked with DSS(d_0/d_{12}).** The digest was injected into a column of Poly-SULFOethyl A equilibrated at a flow rate of 50 $\mu\text{l}/\text{min}$ in buffer, pH 2.7, containing 10% acetonitrile and eluted with a gradient of potassium chloride (gray line) from 0 to 1.0 M. The absorbance (mAU) of the effluent was monitored at 225 nm (black line). The cross-linked peptides were identified in fractions collected across the second peak eluting at 27–40 min.

Analysis of Cross-linked Peptides by Mass Spectrometry—Tryptic digests of protein bands from SDS-PAGE gels were analyzed in a MALDI-TOF-TOF mass spectrometer (Model 4800, ABSciex, Warrington, WA1 1RX, UK) with α -cyano-4-hydroxycinnamic acid as matrix. Peptides were fragmented by collision-induced dissociation with air at a collision energy of 1 kV. Trypsin digests of cross-linked F-ATPases (~ 400 fmol), and fractions of peptides from similar digests that had been obtained by cation exchange chromatography were injected into a nano-scale C_{18} reverse phase column. The eluate was introduced directly into the nanospray interface of a LTQ Orbitrap XL ETD mass spectrometer (Thermo-Fisher Scientific, Hemel Hempstead, UK), operated in data-dependent acquisition mode. Up to 10 of the most abundant precursor ions of known charge states, but not singly charged, were selected and fragmented by collision-induced dissociation. The m/z values of precursor and fragment ions were measured simultaneously in the Orbitrap and ion-trap analyzers, respectively.

Data Analysis—Data files were processed with Proteome Discoverer (Thermo-Fisher Scientific). The coverage of the sequences of the subunits of the F-ATPase by the tryptic peptides was determined by comparison of the sequences of peptides with the mammalian subsection of the non-redundant database of the National Center for Biotechnology Information with MASCOT (25). “Mono-linked” peptides, where only one arm of the bifunctional cross-linking agent reacted with a protein amino group, were identified by comparison of the data with a FASTA database containing the sequences of the subunits of the enzyme. In these comparisons the light and heavy isotopes of the hydrolysis and aminolysis derivatives of mono-linked α -amino and ϵ -amino groups, oxidized methionines, and *S*-propionamido- and *S*-carbamidomethyl derivatives of cysteine were considered as possible modifications with the following parameters: peptide mass tolerance, ± 5 ppm; fragment mass tolerance, ± 0.5 Da; maximum missed cleavages, 2; peptide confidence, at least medium.

Identification of Cross-linked and Loop-linked Peptides—Doublet peaks corresponding to the light and heavy isotopically labeled cross-linked peptides (including loop-linked peptides) were identified from their mass differences with Hekate (26). For the doublets for DSS(d_0/d_{12}) and BS³(d_0/d_{12}) the mass difference was 12.0741 ± 0.0375 , and for DSG(d_0/d_6) and DSSG(d_0/d_6) it was 6.0370 ± 0.0375 Da. No limits were imposed on the intensity ratios of the doublet peaks. To be assigned as an isotopic doublet, peptide ions containing light and heavy isotopes were required to elute within 30 s of each other. The mass threshold for matching the masses of the light isotope peak of cross-linked peptides with their calculated theoretical values was 2 ppm. The accuracy threshold used in the annotation of fragment ions was ± 0.5 Da. The identified cross-links were ranked according to a modified version of Andromeda (26, 27) with fragment ion data from both the light- and heavy-labeled cross-linked peptides.

Mass spectra from cross-linked and loop-linked peptides with a score of >400 were inspected manually. A cross-link was accepted as being significant if both cross-linked peptides had more than five unique fragment ions assigned to them or if the cross-linked peptide had three-five unique fragments ions assigned to one component and more than five to the other. Accepted loop links had three or more unique assigned fragments. Twenty mono-links and six loop links were detected (data not shown). Peptides were discarded when the majority of high intensity fragment ions were not annotated with a theoretical fragment ion from the associated peptide or when fewer than three fragment ions of a peptide component of a cross-link were detected.

Localization of Cross-links in the Structure of the Bovine F-ATPase—A structure of the bovine F_1 - c_8 -peripheral stalk complex was generated from the structures of the bovine F_1 - c_8 -ring (PDB code 2XND (4)), the F_1 -peripheral stalk (PDB code 2WSS (7)), and the peripheral stalk (PDB code 2CLY (8)), and the position of the peripheral stalk was adjusted according a low resolution structure of the intact complex (11). The distances between $C\alpha$ atoms of lysine residues in the model of the bovine F_1 - c_8 -peripheral stalk complex were estimated with PyMOL and Coot (28, 29). For DSS(d_0/d_{12}) and BS³(d_0/d_{12}), the maximum permitted inter- $C\alpha$ distance between connected lysines is 27.4 Å (the 11.4 Å spacer arm plus the length of two lysine side chains, each 6.5 Å, plus twice the coordinate error of 1.5 Å for mobile surface residues). For DSG(d_0/d_6) and DSSG(d_0/d_6) with spacer arms of 7.7 Å, the maximum inter- $C\alpha$ distance is 23.7 Å.

Analysis of Sequences of F-ATPases—Sequences of subunits of F-ATPases were aligned with ClustalW (30). Transmembrane α -helices were predicted with HMMTOP (31), and the secondary structures of membrane extrinsic regions were predicted with PSIPRED (32).

Results

Optimization of Reaction Conditions for Cross-linking the F-ATPase—The concentrations of cross-linkers, and the pH, duration, and temperature of reaction were optimized by varying the conditions and by monitoring the effect of cross-linking on the F-ATPase by SDS-PAGE and blue native-PAGE. The

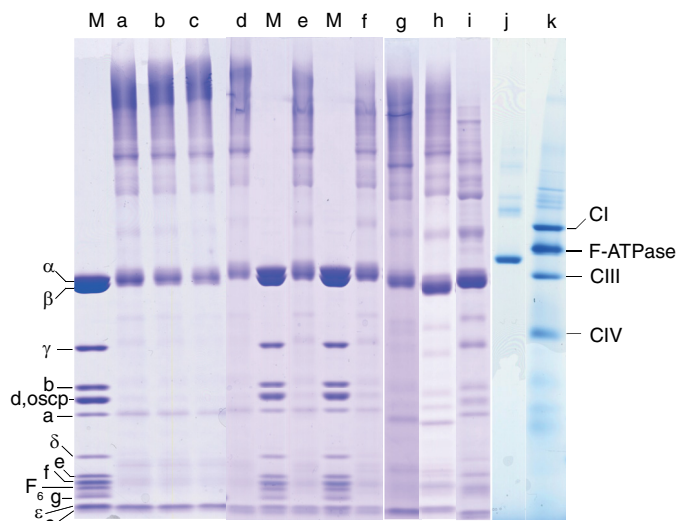


FIGURE 2. Effect of varying the reaction conditions on the cross-linking of the bovine F-ATPase. The enzyme (1.16 mg/ml) was reacted at 37 °C with DSS(d_0/d_{12}) (lanes *a–f*) or $BS^3(d_0/d_{12})$, DSG(d_0/d_6), or DSSG(d_0/d_6) (lanes *g–i*, respectively) at final reagent concentrations of 2 mM. For reference, the molecular weights of subunits α , *oscp*, and ϵ are 55,200, 20,900, and 5,600, respectively. The samples of modified enzyme were analyzed by SDS-PAGE (lanes *a–i*) and by blue native PAGE (lanes *j* and *k*). *M* denotes unreacted enzyme; lanes *a–c*, enzyme reacted with DSS(d_0/d_{12}) for 2, 4, and 20 h; lanes *d–f*, enzyme reacted with DSS(d_0/d_{12}) for 2 h at pH values of 8.0, 7.3, and 6.8; lanes *g–i*, enzyme reacted for 2 h at pH 8.0 with $BS^3(d_0/d_{12})$, DSG(d_0/d_6), or DSSG(d_0/d_6), respectively; lane *j*, enzyme reacted with DSS(d_0/d_{12}) for 2 h at pH 8.0; lane *k*, bovine inner mitochondrial membranes solubilized in the presence of *n*-dodecyl- β -D-maltose-neopentyl glycol. The migration positions of unmodified subunits of the enzyme are indicated on the left and on the right of native respiratory complexes I, III, and IV (*CI*, *CIII*, and *CIV*, respectively).

effect of varying the duration and pH of the reaction of DSS(d_0/d_{12}) with the enzyme is illustrated in Fig. 2 (lanes *a–c* and *d–f*, respectively). The effects of reaction of the enzyme with $BS^3(d_0/d_{12})$, DSG(d_0/d_6), and DSSG(d_0/d_6) for 2 h at pH 8.0 and 37 °C are shown in lanes *g–i* in Fig. 2. The formation of intersubunit cross-links was indicated by the disappearance from the SDS-PAGE gels of the monomeric subunits of the enzyme accompanied by the formation of high molecular weight bands. The optimal conditions were considered to be those where the extent of formation of cross-linked products detected by SDS-PAGE analysis was greatest and the formation of multimeric cross-linked F-ATPase complexes, as detected by blue native-PAGE analysis, was minimal (Fig. 2, lane *j*). Those conditions are 2 μ M F-ATPase (1.16 mg/ml) with 2 mM DSS (d_0/d_{12}) at pH 8.0 for 2 h at 37 °C. In lanes *a–c*, *e*, *f*, and *h* in Fig. 2, it is evident that the α - and γ -subunits were unreactive with DSS(d_0/d_{12}), and in lane *j*, that cross-linking of the enzyme reduced its apparent molecular mass on blue native PAGE gels relative to unreacted enzyme (Fig. 2, lane *k*), presumably because the cross-links make the enzyme more compact.

Characterization of Cross-linked Peptides—The number of cross-links identified in each experiment depended upon how the tryptic peptides were generated and fractionated. Fewer cross-linked pairs were identified in samples processed by SDS-PAGE and in-gel digestion than from other samples that were digested with trypsin and analyzed without any further fractionation, probably because of losses of cross-linked peptides in

the former procedure during their extraction from gels and subsequent processing. However, there was considerable overlap between the sets of cross-linked peptides that were identified by these means. The most effective procedure was that applied to the tryptic digest of the F-ATPase modified with DSS(d_0/d_{12}), where cross-linked peptides were separated from unmodified, mono-linked, and loop-linked peptides by cation exchange chromatography at pH 2.7. At this pH value, cross-linked peptide pairs carry four positive charges (or more if histidine residues are present) and so they bind more strongly to a strong cation exchange resin than unmodified, mono-linked, and loop-linked peptides, which carry a minimum of two positive charges. Thus, the cross-linked peptides were recovered in a separate peak eluting after the less positively charged peptides (Fig. 1). Of the 53 cross-linked peptides identified in this peak (Tables 1 and 2), 30 contained intrasubunit cross-links, and 23 had intersubunit cross-links. In other experiments where the ion exchange step was omitted, 28 peptides cross-linked with DSS were recovered, and 24, 14, and 17 peptides cross-linked with BS^3 , DSG, and DSSG were recovered, respectively. There was no significant difference between the number of cross-linked peptides recovered from the membrane subunits of the F-ATPase reacted with the membrane-permeable reagents, DSS and DSG, and with the membrane-impermeable reagents, BS^3 and DSSG.

Cross-links in the Membrane Extrinsic Region of the F-ATPase—Forty-four cross-linked peptide pairs were identified as originating from membrane-extrinsic subunits of the enzyme. They are summarized in Table 1 together with the $C\alpha$ distances between the cross-linked lysine residues measured in the structure of the bovine F-ATPase, and the corresponding mass spectrometry data are summarized in Table 2. The lengths of cross-linkers are given in the experimental section. In 38 of them both lysines are resolved in the structure, and the formation of the cross-links is compatible with the inter- $C\alpha$ distances. For a 39th cross-link between α Lys-455 and Lys-24 in subunit *d*, the inter- $C\alpha$ distance of 32.3 Å is only slightly above the maximum value of 27.4 Å, and a minor conformational change in the determined structure of the enzyme would allow this cross-link to form. In two other cross-links between the F_1 domain and the peripheral stalk, one of the reacted lysine residues is in a region that is locally unresolved in the structure, although adjacent structural elements are well defined. One such cross-link bridges between unresolved residue β Lys-9 in the N-terminal region of the subunit and residue β Lys-78, which is resolved in the six-stranded β -barrel that forms part of the “crown” of the F_1 domain. The $C\alpha$ distances between the resolved residue β Thr-13, which is close to β Lys-9 in the sequence of the subunit, and β Lys-78 are 10 Å, 10 Å, and 10.2 Å in the β_{DP} -, β_{TP} -, and β_E -subunits, respectively. Therefore, the formation of a cross-link bridging between β Lys-9 and β Lys-78 is compatible with the structure. The second cross-link involves the unresolved residue Lys-2 in subunit F_6 and the resolved residue Lys-191 in subunit *b*. It is clear from the structure of the enzyme that residue Lys-2 in subunit F_6 and residue Lys-191 in the C-terminal region of subunit *b* are in close proximity (the estimated distance is \sim 25 Å), and the formation of this cross-link is consistent with this conclusion.

Membrane Subunits of Bovine F-ATPase

TABLE 1

Cross-linked tryptic peptides in the membrane extrinsic region of the bovine F-ATPase

The cross-links were produced by reaction of the enzyme with DSS(d_0/d_{12}), and the peptides were fractionated by ion exchange chromatography.

Subunits	Cross-linked sequences	Lys-Lys ^a	C α -C α ^b
α - α	VVDALGNAIDG K GPIGSK-STVAQLV K R	118–218 ^{c,d}	14.9
α - α	GPIG S KAR-DNG K HALIIYDDL S K	124–262 ^{c,e}	17.6
α - α	VGL K APGIIPRISVR-RFNDGTDE K K	132–196	25.4
α - α	FNDGTDE K K-DNG K HALIIYDDL S K	196–262 ^{c,d}	7.4
α - α	FNDGTDE K K-TDG K I SEESDAK	196–488	19.3
α - α	AM K QVAGTMK-TDG K I SEESDAK	384–488 ^{c,d,e}	8.8
α - α	GYLD K LEPSK-L K EIVTNFLAGFEA	455–498 ^{c,d,e}	15.1
α - α	FENAFLSHVISQH Q GALL S KIR-TDG K I SEESDAK	482–488 ^{d,e}	8.4
α - β	VVDALGNAIDG K GPIGSK-ITTT K K	118–304 ^{c,d,e}	16.8
α - β	RSTVAQLV K R-ITTT K K	218–304 ^{c,d,e}	15.0
α - γ	VGSAAQTRAM K QVAGTMK-ATL K DI T R	384–4	39.1
α -oscp	LI K EGDIVKR-YVDM S A K TK	83–176	21.0
α -b	VVDALGNAIDG K GPIGSK-EV K NR	118–152	21.6
α -d	GYLD K LEPSK-N Q KAVAN S LK	455–24	32.3
β - β	AAQASPS P KAGATTGR-G Q KVLD S GAPIR	9–78 ^d	– ^f
β - β	VVDLLAPYA K G G K-LVPL K ETIK	152–439	18.2
β - β	FLSQPFQVAEVFT G HL G KLVPL K -AD K LAE H S	430–476 ^d	18.5
β - δ	K IQR-AN L E K AQ S ELLGADEATR	413–114	57.3
γ - γ	ATL K DI T R-SI K NI Q K	4–14	15.3
γ - γ	SI K NI Q K-IT K SM K	14–21 ^d	10.8
γ - γ	ADI K TPEDK-SEANLAAAG K EV K	58–101	14.3
γ - ϵ	MVAA A K Y AR-ANAM K TS G STIK	30–36 ^{c,d,e}	14.4
γ - ϵ	EL K PAR-ANAM K TS G STIK	39–36	16.3
γ - ϵ	THSDQFLVTF F KEVGR-IV K V K	129–46 ^e	10.5
δ - ϵ	AN L E K AQ S ELLGADEATR-YS Q ICAKAVR	114–20 ^{c,e}	12.7
δ - ϵ	AN L E K AQ S ELLGADEATR-TE F KANAMK	114–31 ^e	21.0
δ - ϵ	AN L E K AQ S ELLGADEATR-DAL K TE F KANAMK	144–27	18.3
ϵ - ϵ	YS Q ICAKAVR-TE F KANAMK	20–31 ^{c,d}	13.0
ϵ - ϵ	YS Q ICAKAVR-ANAM K TS G STIK	20–36 ^c	13.8
oscp-oscp	VGQIL K EPK-SV K V K	47–65	15.5
oscp-oscp	EP K MAASLLNPYV K -V K SLSDMTAK	50–67	16.5
oscp-oscp	EP K MAASLLNPYV K -SLSDMT A KEK	50–75 ^c	16.3
oscp-oscp	MAASLLNPYV K R-V K SLSDMTAK	61–67 ^e	11.0
b-b	VVQ S ISAQ Q E K ETIAK-CIADL K LL S K	191–202 ^d	16.3
b-d	QIQDAIDME K SQQALV Q K-SCAEFL T Q S K T R	112–108 ^d	11.8
b-F ₆	VVQ S ISAQ Q E K ETIAK-N K ELDPV Q K	191–2	– ^g
b-F ₆	VVQ S ISAQ Q E K ETIAK-LFV D KIR	191–14	14.7
d-d	K LAL K -LATL P E K PPAIDWAY K	4–47 ^{c,e}	12.9
d-d	K LAL K -FNAL K VPI P EDK	4–77	18.3
d-d	LATL P E K PPAIDWAY K -FNAL K VPI P EDK	47–77	13.0
d-d	ANVA K AGLVDD F E K - K FNAL K	62–72 ^d	16.0
d-d	AGLVDD F E K K-FNAL K VPI P EDK	71–77	12.0
d-d	SCAEFL T Q S K T R-I Q E Y E K E L E K	108–116	12.2
d-F ₆	ANVA K AGLVDD F E K - L K Q MY G K	62–47	17.8

^a Sequence numbers of cross-linked lysines. The hyphens separate the two peptides, and cross-linked residues are bold.

^b Measured in Å in the structure of the bovine F₁-c₈-peripheral stalk complex.

^c Cross-link also found in bovine F-ATPase modified with DSG(d_0/d_6).

^d Cross-link also found in bovine F-ATPase modified with BS³(d_0/d_{12}).

^e Cross-link also found in bovine F-ATPase modified with DSSG(d_0/d_6).

^f The N-terminal region of β -subunits is disordered.

^g Residue 2 of subunit F₆ is not resolved.

Three other cross-links are incompatible with the structure of the monomeric bovine F-ATPase, and each was observed once only (see Table 1). One of them bridges between β Lys-413 and δ Lys-114, whereas the C α distance between the two lysine residues in the structure is 57.3 Å. This cross-link is likely to have formed between two different F-ATPase complexes, and the presence of a small amount of the oligomeric complex in the native gel of the modified complex (Fig. 2, lane j) is consistent with this suggestion. Another incompatible cross-link bridges between α Lys-132 and α Lys-196, two surface residues in the nucleotide binding domain of the subunit. Although the inter-C α value given in Table 1 is apparently within the range of acceptable distances, this distance has been measured along the direct path between the two C α -atoms, which is impeded by a loop involving residues 309–321 of the α -subunit, and the unimpeded C α distance is considerably longer. The third structurally incompatible cross-link is between α Lys-384 and γ Lys-4. The former residue is exposed at the entrances to cat-

alytic interfaces between the α -subunits and the adjacent β -subunit, whereas the latter residue is in the N-terminal α -helix of the γ -subunit. This α -helix is one of the two α -helical elements in the central shaft of the rotor found in the aqueous cavity in the core of the F₁ domain. In one of the three catalytic α - β interfaces, between α_{DP} and β_{DP} , there is a direct unimpeded line of sight between the two residues, but the gap narrows to ~6 Å, and the inter-C α distance is 38.4 Å. These last two structurally incompatible cross-links could only have formed by reaction with disrupted F-ATPase complexes. Despite these three aberrant cross-links, the overwhelming majority, 93%, of the observed linkages were compatible with the atomic structure of the F-ATPase. Their main value is that they provide reassurance that any cross-links observed in regions of the F-ATPase that are not represented in the current structural model are likely to have validity and that they represent contributions toward defining the organization of subunits in the unresolved region.

TABLE 2
Mass spectrometric characterization of cross-linked tryptic peptides in the membrane extrinsic region of the bovine F-ATPase

 The cross-links were produced by reaction of the enzyme with DSS(d_0/d_{12}), and the peptides were fractionated by ion exchange chromatography.

Subunits	Lys-Lys ^a	Score	<i>m/z</i>	<i>Da</i> MH ⁺	Charge	ppm
α - α	118–218 ^{b,c}	758	950.54217	2849.61197	3	0.89
α - α	124–262 ^{b,d}	738	875.47418	2624.40800	3	1.45
α - α	132–196	450	974.88971	2922.65459	3	0.78
α - α	196–262 ^{b,c}	691	964.81470	2892.42956	3	1.19
α - α	196–488	627	824.05456	2470.14914	3	0.98
α - α	384–488 ^{b,c,d}	839	827.74683	2481.22595	3	1.95
α - α	455–498 ^{b,c,d}	486	946.84473	2838.51965	3	0.76
α - α	482–488 ^{c,d}	635	964.50415	3854.99479	4	0.65
α - β	118–304 ^{b,c,d}	852	847.15118	2539.43900	3	1.93
α - β	218–304 ^{b,c,d}	436	497.30722	1986.20707	4	0.04
α - γ	384–4	615	723.14758	2889.56851	4	1.26
α -oscp	83–176	573	784.10754	2350.30808	3	1.30
α -b	118–152	725	831.79480	2493.36986	3	1.11
α -d	455–24	745	787.10058	2359.28720	3	0.20
β - β	9–78 ^c	478	712.88782	2848.52947	4	0.69
β - β	152–439	496	836.84064	2508.50738	3	0.92
β - β	430–476 ^c	707	923.74963	3691.976671	4	0.91
β - δ	413–114	621	890.14807	2668.42967	3	1.22
γ - γ	4–14	782	629.04211	1885.11179	3	0.05
γ - γ	14–21 ^c	480	558.99921	1674.98309	3	0.49
γ - γ	58–101	682	838.11029	2512.31633	3	0.91
γ - ϵ	30–36 ^{b,c,d}	572	776.08063	2326.22735	3	0.69
γ - ϵ	39–36	512	692.37775	2075.11871	3	1.07
γ - ϵ	129–46 ^d	595	829.80475	2487.39971	3	1.11
δ - ϵ	114–20 ^{b,d}	645	1107.23755	3319.69811	3	0.92
δ - ϵ	114–31 ^d	575	1055.20410	3163.59776	3	1.21
δ - ϵ	144–27	579	902.46393	3606.83391	4	0.55
ϵ - ϵ	20–31 ^{c,d}	899	791.40918	2372.21300	3	1.22
ϵ - ϵ	20–36 ^d	711	847.77789	2541.31913	3	1.09
oscp-oscp	47–65	768	570.35724	1709.05718	3	0.04
oscp-oscp	50–67	949	926.50006	2777.48564	3	1.05
oscp-oscp	50–75 ^d	1083	936.49115	2807.45891	3	0.71
oscp-oscp	61–67 ^d	577	860.47052	2579.39702	3	1.35
b-b	191–202 ^c	817	1019.57013	3056.69585	3	1.54
b-d	112–108 ^c	1211	910.21136	3637.82363	4	0.99
b-F ₆	191–2	816	989.54022	2966.60612	3	0.57
b-F ₆	191–14	669	929.52832	2786.57042	3	1.52
d-d	4–47 ^{b,d}	620	672.13818	2685.53091	4	1.62
d-d	4–77	671	694.08649	2080.24493	3	1.60
d-d	47–77	559	871.72638	3483.88371	4	0.68
d-d	62–72 ^c	622	778.76239	2334.27263	3	0.98
d-d	71–77	712	877.14307	2629.41467	3	0.90
d-d	108–116	839	958.48065	2873.42741	3	1.29
d-F ₆	62–47	690	827.77423	2481.30815	3	0.97

^a Sequence numbers of cross-linked lysines.

^b Cross-link also found in bovine F-ATPase modified with DSG(d_0/d_6).

^c Cross-link also found in bovine F-ATPase modified with BS³(d_0/d_{12}).

^d Cross-link also found in bovine F-ATPase modified with DSSG(d_0/d_6).

Cross-links in the Membrane Domain of the F-ATPase—Eight intersubunit and four intrasubunit cross-links were identified among the tryptic peptides from the F-ATPase that had been cross-linked with the four reagents. The majority of them were identified in the digest of the DSS cross-linked enzyme that was fractionated by ion exchange chromatography. They are summarized in Table 3, and the corresponding mass spectrometry data are summarized in Table 4.

Three of the intersubunit cross-links were between subunit ATP8 and components of the peripheral stalk domain. One of them links residue Lys-54 of subunit ATP8 to residue Lys-73 of the F₆ subunit. The two others involve links from residue Lys-46 of ATP8, one to residue Lys-120 of subunit b and the other to residue Lys-24 of subunit d (Fig. 3).

Five of the intersubunit cross-links involved lysine residues in the five supernumerary subunits e, f, g, DAPIT, and 6.8PL (see Fig. 4). All fall in regions of the proteins that are predicted to be membrane extrinsic. Three involve links between residue Lys-49 in the C-terminal region of the 6.8PL subunit with lysine residues in the

TABLE 3
Cross-links to tryptic peptides in the subunits of the membrane intrinsic region of the bovine F-ATPase

Subunits	Cross-linked sequences	Lys-Lys ^a
e-e	LAAE E KK-DEQ K R	47–54 ^{b,c,d,e}
e-e	LAAE E KKK-RDEQ K R	48–54 ^{b,c,d,e}
e-f	LAAE E KK-K Y H	47–85 ^{b,c,d,e}
f-f	E KK-LLE V KL G ELPS W ILMR	9–15 ^{b,c,d,e}
f-g	LLE V KL G ELPS W ILMR-T G S F K Q L T V K	15–65 ^e
ATP8-b	MLK Q NT P W E T K -S Q AL V Q K R	46–120 ^b
ATP8-d	MLK Q NT P W E T K -N Q KAVAN S L K	46–24 ^b
ATP8-F ₆	Q N T P W E T K -F E V E K P Q S	54–73 ^{b,e}
6.8PL-6.8PL	S A D K R-AL K ASSA P A H G H H	43–49 ^{b,e}
6.8PL-e	AL K ASSA P A H G H H-DE Q K R	49–54 ^b
6.8PL-f	AL K ASSA P A H G H H-EL K H E R	49–79 ^b
6.8PL-DAPIT	AL K ASSA P A H G H H-TP A V K A T	49–55 ^b

^a Sequence numbers of cross-linked lysines. The hyphens separate the two peptides, and the cross-linked residues are bold.

^b Cross-links identified in F-ATPase reacted with DSS(d_0/d_{12}).

^c Cross-links identified in F-ATPase reacted with DSG(d_0/d_6).

^d Cross-links identified in F-ATPase reacted with DSSG(d_0/d_6).

^e Cross-links identified in F-ATPase reacted with BS³(d_0/d_{12}).

C-terminal regions of the DAPIT, e, and f subunits. Other cross-links bridge between the C-terminal regions of subunits e and f and the N-terminal regions of subunits f and g.

Membrane Subunits of Bovine F-ATPase

TABLE 4

Mass spectrometric characterization of cross-linked tryptic peptides in the subunits of the membrane intrinsic region of the bovine F-ATPase

Subunits	Lys-Lys ^a	Score	<i>m/z</i>	MH ⁺	Charge	ppm
				<i>Da</i>		
e-e	47–54 ^{b,c,d,e}	927	800.93109	1600.85491	2	0.53
e-e	48–54 ^{b,c,d,e}	775	629.02154	1885.05008	3	0.03
e-f	47–85 ^{b,c,d,e}	765	686.87793	1372.74859	2	1.10
f-f	9–15 ^{b,c,d,e}	1013	813.47479	2438.40983	3	0.30
f-g	15–65 ^e	687	1048.27112	3142.79880	3	0.57
ATP8-b	46–120 ^b	548	862.79572	2586.37259	3	0.68
ATP8-d	46–24 ^b	868	862.46423	2585.37815	3	0.99
ATP8-F ₆	54–73 ^{b,e}	633	873.44446	2618.31882	3	1.97
6.8PL-6.8PL	43–49 ^{b,e}	693	690.02801	2068.06949	3	0.61
6.8PL-e	49–54 ^b	504	542.53105	2167.09878	4	0.69
6.8PL-f	49–79 ^b	422	576.55573	2303.20107	4	0.33
6.8PL-DAPIT	49–55 ^b	560	727.05920	2179.16306	3	0.58

^a Sequence numbers of cross-linked lysines.

^b Cross-links identified in F-ATPase reacted with DSS(*d*₀*d*₁₂).

^c Cross-links identified in F-ATPase reacted with DSG(*d*₀*d*₆).

^d Cross-links identified in F-ATPase reacted with DSSG(*d*₀*d*₆).

^e Cross-links identified in F-ATPase reacted with BS³(*d*₀*d*₁₂).

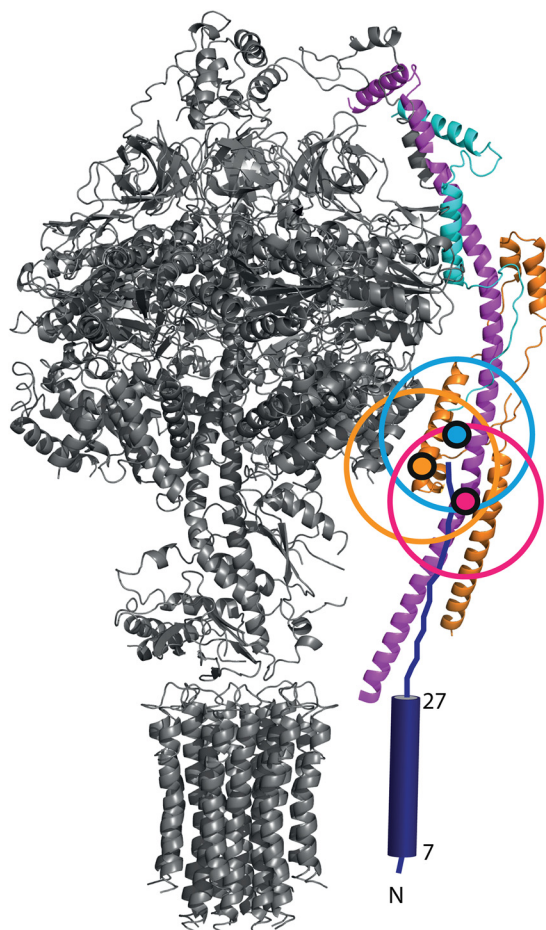


FIGURE 3. Intersubunit cross-links between the C-terminal region of mitochondria-encoded subunit ATP8 and nuclear encoded subunits b, d, and F₆ in the structure of the bovine F-ATPase. The structures of the membrane extrinsic F₁ domain and the attached oscp (top) and the C₈-ring in the membrane domain of the enzyme (bottom) are shown in black. In the peripheral stalk of the complex (right), the membrane extrinsic region of subunit b is magenta, subunit F₆ is blue, and subunit d is orange. Subunit ATP8 is deep blue, and its predicted transmembrane α -helix from residues 8–29 is depicted as a cylinder. Except for the c-ring, the region occupied by membrane components of the enzyme is not shown. The secondary structure of residues 29–66 of subunit ATP8 is not known, and this region is shown in an extended form reaching up so as to place lysine residues 46 and 54 in the vicinity of the residues to which they are cross-linked, residues 120, 24, and 73 (indicated by the magenta, orange, and blue dots in subunits b, d, and F₆, respectively). The colored circles around each dot have a diameter of 20 Å, and they represent the region in which each cross-linked residue in ATP8 is likely to be found in the structure.

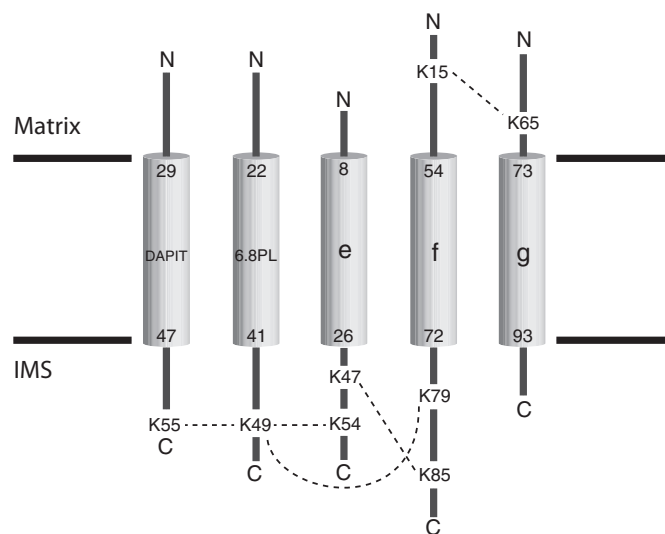


FIGURE 4. Intersubunit cross-links detected in the nuclear encoded supernumerary subunits of the bovine F-ATPase. The cylinders represent the transmembrane α -helices predicted to be present in each of subunits e, f, g, DAPIT, and 6.8PL. The positions of the α -helices in the sequences of the subunits are indicated by the numbers at the top and bottom of each cylinder. The dashed lines represent the intersubunit cross-links, introduced by reaction of the bifunctional cross-linking agents with the numbered lysine residues in the N- and C-terminal regions of each subunit. IMS, intermembrane space.

Discussion

Involvement of Subunit ATP8 in the Bovine Peripheral Stalk—Since its discovery as a subunit of the bovine and yeast F-ATPases (12, 33, 34), subunit ATP8 (also known as A6L in mammals and Aap1 in *Saccharomyces cerevisiae*) has remained a rather mysterious component of the enzyme complex. It is not found in eubacterial and chloroplast enzymes, and therefore, it was classified as a supernumerary subunit, apparently not required for the core ATP synthetic and hydrolytic functions of F-ATPases. The subunit is encoded in the mitochondrial DNA of many, but not all, eukaryotic species (35), and in mammals, the genes for ATP8 and ATPase-6 (or subunit a) overlap (12, 36). The bovine protein is probably folded into a single transmembrane α -helix from residues 8–29 followed by a hydrophilic extension up to its C terminus at residue 66 (Fig. 5A). This region from residue 30 to 66 is predicted to have an

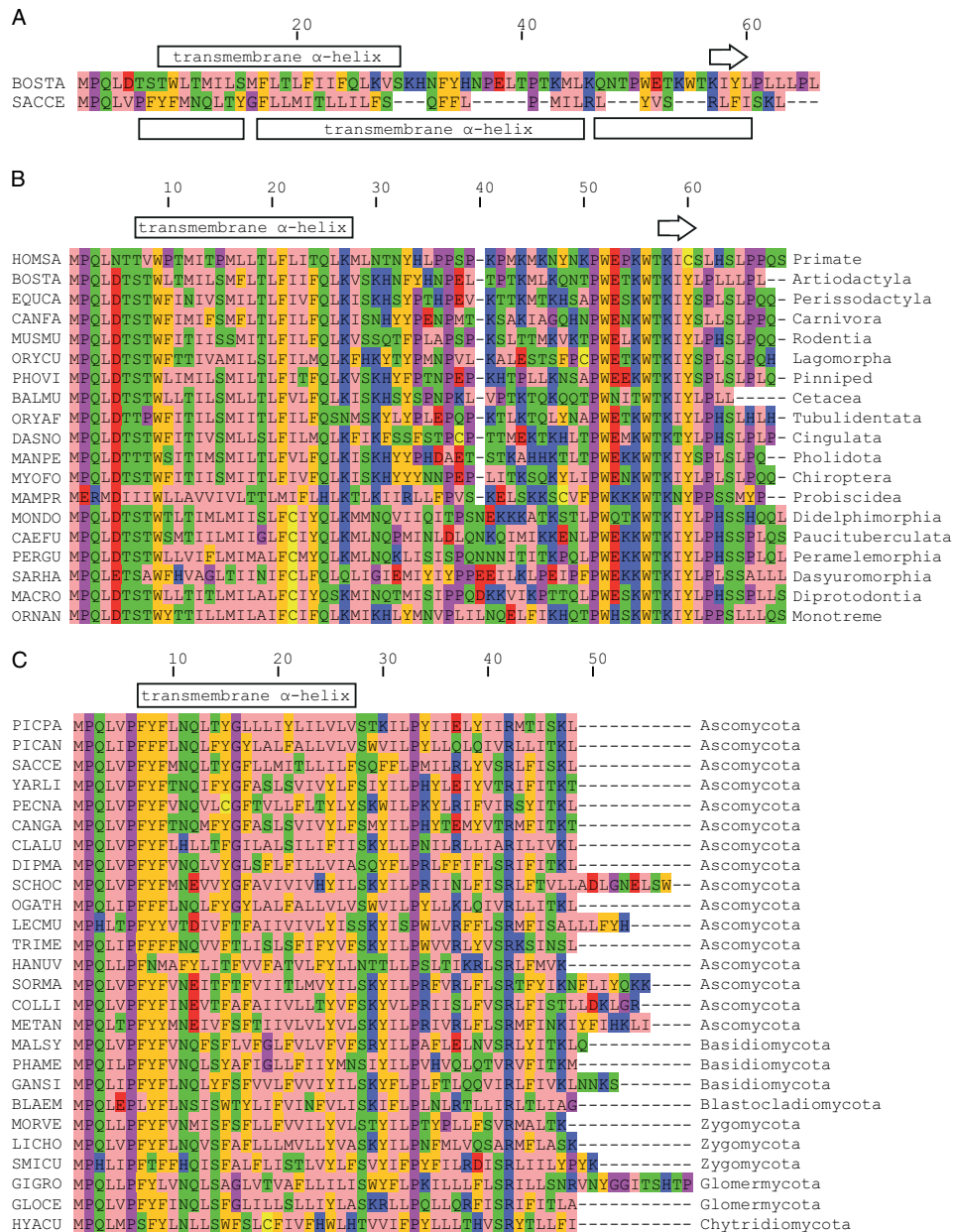


FIGURE 5. Conservation of sequences of ATP8 subunits. Residues are colored as follows: pink, hydrophobic; orange, aromatic; blue, basic; red, acidic; green, hydrophilic; magenta, proline and glycine. Yellow denotes cysteine residues. A, comparison of the sequences of the bovine and yeast ATP8 subunits. The predicted secondary structure of the bovine protein is shown above the sequences. The arrow represents a short predicted β -strand. The regions before, between, and after the α -helices and β -sheet are predicted to be extended. BOSTA, *Bos taurus*; SACCE, *S. cerevisiae*. B and C, conservation of sequences of selected mammalian and fungal ATP8 subunits. In B and C, the orders represented by the species are shown on the right. B: HOMSA, *Homo sapiens*; BOSTA, *B. taurus*; EQUCA, *Equus caballus* (horse); CANFA, *Canis lupus familiaris* (dog); MUSMU, *Mus musculus* (mouse); ORYCU, *Oryctolagus cuniculus* (rabbit); PHOVI, *Phoca vitulina* (harbor seal); BALMU, *Balaenoptera musculus* (blue whale); ORYAF, *Orycteropus afer* (aardvark); DANO, *Dasybus novemcinctus* (nine-banded armadillo); MANPE, *Manis pentadactyla* (Chinese pangolin); MYOFO, *Myotis formosus* (Hodgson's bat); MAMPR, *Mammuthus primigenius* (woolly mammoth); MONDO, *Monodelphis domestica* (gray short tailed opossum); CAEFU, *Caenolestes fuliginosus* (silky shrew opossum); PERGU, *Perameles gunnii* (eastern barred bandicoot); SARHA, *Sarcophilus harrisii* (Tasmanian devil); MACRO, *Macropus robustus* (common wallaroo); ORNAN, *Ornithorhynchus anatinus* (duck-billed platypus). C: PICPA, *Pichia pastoris*; PICAN, *Pichia angusta*; SACCE, *S. cerevisiae*; YARLI, *Yarrowia lipolytica*; PECNA, *Pneumocystis carinii*; CANGA, *Candida galli*; CLALU, *Clavospora lusitanae*; DIPMA, *Dipodascus magnusii*; SCHOC, *Schizosaccharomyces octosporus*; OGATH, *Ogataea thermophila*; LECMU, *Lecanicillium muscarium*; TRIME, *Trichophyton mentagrophytes*; HANUV, *Hanseniaspora uvarum*; SORMA, *Sordaria macrospora*; COLLI, *Colletotrichum lindemuthianum*; METAN, *Metarhizium anisopliae*; MALSU, *Malassezia sympodialis*; PHAME, *Phakopsora meibomia*; GANSI, *Ganoderma sinense*; BLAEM, *Blastocladiella emersonii*; MORVE, *Mortierella verticillata*; LICHO, *Lichtheimia hongkongensis*; SMICU, *Smittium culisetae*; GIGRO, *Gigaspora rosea*; GLOCE, *Glomus cerebriforme*; HYACU, *Hyaloraphidium curvatum*.

extended conformation, except for residues 57–61, which may form a short β -sheet. The region consisting of residues 51–63 is well conserved in mammals (Fig. 5B). In contrast, subunit ATP8 in *S. cerevisiae* has a C-terminal extension that is predicted to be mostly α -helical. It is significantly shorter and poorly related

to the same region of the mammalian proteins, although the sequences of ATP8 proteins are well conserved among the fungi (Fig. 5C). On the basis of cysteine scanning mutagenesis and reaction with fluorescein-5-maleimide, residues 1–14 of yeast ATP8 have been proposed to be exposed to the intermem-

Membrane Subunits of Bovine F-ATPase

brane space followed by a transmembrane α -helix from residues 15–35 (37). A short β -strand is predicted around residue Arg-42, and this residue is conserved throughout fungi (Fig. 5C). Despite these differences, proteolytic digestion studies conducted on bovine mitochondrial membranes (38, 39) and cross-linking studies on the yeast enzyme (40) have shown that the bovine and yeast proteins have a common topography with

their N-terminal regions in the intermembrane space and their C-terminal regions on the matrix side of the inner mitochondrial membrane.

In the current work new information about the location of bovine subunit ATP8 in the F-ATPase has come from an extensive study of covalent cross-linking conducted on the intact purified enzyme with bi-functional agents. Among the many



identified cross-links, residues Lys-46 and Lys-54 of ATP8 were found to be linked to three lysine residues, one in each of subunits b, d, and F₆ in the peripheral stalk of the enzyme. These cross-links confirm that the C-terminal region of bovine ATP8 is exposed in the matrix of the organelle, and they demonstrate that this region of ATP8 is in the vicinity of the peripheral stalk. The shorter and poorly related C-terminal region of yeast subunit ATP8 has been proposed to interact with subunits b and d in the yeast enzyme (37). Two of the cross-links in the bovine enzyme involve the structurally defined residues Lys-120 and Lys-24 of subunits b and d, respectively, both of which are found ~60 Å from the membrane domain of the enzyme. Therefore, residues Lys-46 and Lys-54 of ATP8 are nearby (see Fig. 3), and the C-terminal region of bovine subunit ATP8 extends ~60–70 Å upwards from the membrane domain, probably along the axis of the peripheral stalk defined by the long α-helix in subunit b. The third cross-link is between residue Lys-54 in ATP8 and residue Lys-73 in subunit F₆ (Fig. 3). Bovine subunit F₆ is 76 amino acids long, and in the peripheral stalk, it is folded into two α-helices from residues 4–25 and 33–51 linked by an extended loop region from residues 26–32. Residue 51 is followed by an extended region, which is resolved up to residue Glu-69. The cross-linked residue Lys-73 of F₆ is nearby and is estimated to be ~70 Å from the surface of the membrane domain of the enzyme, in accordance with the position deduced from the structurally defined lysine residues in subunits b and d. The only known human pathogenic mutation specific to subunit ATP8 is associated with infantile cardiomyopathy, and it leads to the truncation of the subunit at residue 54 and impairment of ATP synthesis (41). Therefore, in mammalian mitochondrial enzymes subunit ATP8 appears to have a fundamental role in either the synthesis of ATP by mitochondrial F-ATPases or the assembly of the complex or both. If the C-terminal region of subunit ATP8 is, as proposed, an intrinsic component of the peripheral stalk, truncation of the subunit would disrupt the integrity of the peripheral stalk and impair ATP synthesis by uncoupling the catalytic sites in the F₁ domain from the proton motive force, generated across the inner mitochondrial membrane by respiration. Similar proposals have been made that the yeast ATP8 subunit is a component of the peripheral stalk of the yeast F-ATPase (37, 40) and that it is required for the assembly of the complex (42, 43). Thus, despite significant differences in the lengths and sequences of mamma-

lian and yeast ATP8 subunits, it is likely that they have related roles in the enzyme complexes.

Organization of Supernumerary Subunits—The presence of the supernumerary subunits e, f, and g in the membrane domains of F-ATPases was demonstrated first in the bovine enzyme (2, 13) and subsequently in the enzyme from *S. cerevisiae* (15, 44). All three subunits are predicted to contain a single transmembrane α-helix (see Fig. 4), and the sequences of the bovine and yeast e, f, and g subunits are conserved or conservatively substituted in 26%, 34%, and 46% of their residues, respectively. The predicted secondary structures of the bovine and yeast orthologs are similar but not entirely concordant. Since their discovery, the roles of the yeast subunits have been studied much more extensively than their bovine orthologs. Yeast subunits e and g are involved in the formation of dimers of the enzyme in the mitochondrial cristae (15, 45, 46), and they are oriented with their N-terminal regions in the mitochondrial matrix and their C-terminal regions in the intermembrane space of the organelle (37, 47). A GXXXG sequence motif in residues 14–18 of the yeast e-subunit forms a homodimeric α-helical coiled-coil involved in holding two F-ATPase complexes together (45). However, the motif is not conserved in the bovine protein. Deletion of either subunit e or subunit g leads to severe disruption of the structure of the mitochondrial cristae, but neither subunit is required for the formation of an enzymatically active complex (15, 48). Like subunits e and g, subunit f is oriented with its N- and C-terminal regions in the mitochondrial matrix and the intermembrane space, respectively (37, 47, 49), but in contrast to subunits e and g, deletion of subunit f disrupted both the assembly and the activity of the complex (44). In addition to subunits ATP8, e, f, and g, the membrane domain of the bovine enzyme also contains two additional subunits, DAPIT and 6.8PL (14, 50), that have been identified also in the human enzyme (51). They are less tightly associated with the bovine complex than the other supernumerary subunits, and they require the presence of phospholipids to remain bound to the complex (14). Subunit DAPIT is encoded only in the genomes of metazoans (Fig. 6), and subunit 6.8PL is restricted to vertebrates (Fig. 7), and so neither subunit is a component of the yeast enzyme. Both have a single predicted transmembrane α-helix (Fig. 4). Conversely, the membrane domains of the yeast F-ATPase additionally contain subunits j (also called i) and k (15, 52, 53), and a recently discovered sub-

FIGURE 6. Conservation of the sequences of the DAPIT subunit in metazoan F-ATPases. For details of the color scheme see the legend to Fig. 5. *HOMSA*, *H. sapiens* (human); *BOSTA*, *B. taurus* (cow); *SUSSC*, *Sus scrofa* (wild boar); *NOMLE*, *Nomascus leucogenys* (Northern white-cheeked gibbon); *PAPAN*, *Papio anubis* (olive baboon); *PANHO*, *Panthalops hodgsonii* (chiru); *VICPA*, *Vicugna pacos* (alpaca); *EQUCA*, *E. caballus* (horse); *FELCA*, *Felis catus* (cat); *RATNO*, *Rattus norvegicus* (rat); *MUSMU*, *M. musculus* (mouse); *ICTTR*, *Ictidomys tridecemlineatus* (squirrel); *CHILA*, *Chinchilla lanigera* (long-tailed chinchilla); *OTOGA*, *Otolemur garnettii* (Garnett's greater bushbaby); *MONDO*, *M. domestica* (gray short-tailed opossum); *ORNAN*, *O. anatinus* (duckbill platypus); *TURTR*, *Tursiops truncatus* (Atlantic bottle-nosed dolphin); *GALGA*, *Gallus gallus* (chicken); *MELGA*, *Meleagris gallopavo* (common turkey); *FALPE*, *Falco peregrinus* (peregrine falcon); *ANAPL*, *Anas platyrhynchos* (domestic duck); *TAEGU*, *Taeniopygia guttata* (zebra finch); *MELUN*, *Melospittacus undulatus* (budgerigar); *PELSI*, *Pelodiscus sinensis* (Chinese softshell turtle); *ALLMI*, *Alligator mississippiensis* (American alligator); *XENTR*, *Xenopus tropicalis* (clawed frog); *RANCA*, *Rana catesbeiana* (American bullfrog); *SALSA*, *Salmo salar* (salmon); *LATCH*, *Latimeria chalumnae* (West Indian ocean coelacanth); *DANRE*, *Danio rerio* (zebrafish); *CIOIN*, *Ciona intestinalis* (transparent sea squirt); *ZOONE*, *Zootermopsis nevadensis* (termite); *TRICA*, *Tribolium castaneum* (red flour beetle); *RIPPE*, *Riptortus pedestris* (bean bug); *DENPO*, *Dendroctonus ponderosae* (mountain pine beetle); *CERCA*, *Ceratitis capitata* (medfly); *NEOBU*, *Neobellieria bullata* (flesh fly); *ACRPI*, *Acyrtosiphon pisum* (pea aphid); *ANOSI*, *Anopheles sinensis* (mosquito); *AEDAE*, *Aedes aegypti* (yellow fever mosquito); *CULQU*, *Culex quinquefasciatus* (house mosquito); *MUSDO*, *Musca domestica* (housefly); *NASVI*, *Nasonia vitripennis* (jewel wasp); *DROME*, *Drosophila melanogaster* (fruit fly); *CERBI*, *Cerapachys biroi* (clonal raider ant); *MICDE*, *Microplitis demolitor* (parasitic wasp); *BOMMO*, *Bombyx mori* (silkworm); *BOMTE*, *Bombus terrestris* (bumblebee); *APIFL*, *Apis florea* (dwarf honey bee); *PAPXU*, *Papilio xuthus* (Asian swallowtail); *DANPL*, *Danaus plexippus* (monarch butterfly); *DAPPU*, *Daphnia pulex* (water flea); *STEMI*, *Stegodyphus mimosarum* (social spider); *IXOSC*, *Ixodes scapularis* (tick); *METOC*, *Metaseiulus occidentalis* (mite); *SCHJA*, *Schistosoma japonicum* (blood fluke); *AMPQU*, *Amphimedon queenslandica* (sea sponge); *CAPOW*, *Capsaspora owczarzaki* (filasterean amoeba).

Membrane Subunits of Bovine F-ATPase



FIGURE 7. Conservation of the sequences of the 6.8PL subunit in vertebrate F-ATPases. For details of the color scheme, see the legend to Fig. 5. HOMSA, *H. sapiens* (human); BOSTA, *B. taurus* (cow); PANTR, *Pan troglodytes* (chimpanzee); RATNO, *R. norvegicus* (rat); MUSMU, *M. musculus* (mouse); PTEAL, *Pteropus alecto* (black flying fox); SORAR, *Sorex araneus* (shrew); SUSSC, *S. scrofa* (wild boar); ORYCU, *O. cuniculus* (rabbit); MONDE, *M. domestica* (gray short-tailed opossum); ORNAN, *O. anatinus* (duckbill platypus); TURTR, *T. truncatus* (bottle nose dolphin); GALGA, *G. gallus* (chicken); ANAPL, *A. platyrhynchos* (domestic duck); NIPNI, *Nipponia nippon* (crested ibis); PYGAD, *Pygoscelis adeliae* (Adelie penguin); MANVI, *Manacus vitellinus* (golden-collared manakin); MERNU, *Merops nubicus* (northern carmine bee eater); COLLI, *Columba livia* (pigeon); PHACA, *Phalacrocorax carbo* (cormorant); MELUN, *M. undulatus* (budgerigar); OPIHO, *Opisthocomus hoazin* (hoatzin); PELCR, *Pelecanus crispus* (pelican); LEPDI, *Leptosomus discolor* (cuckoo); STRAU, *Struthio camelus australis* (ostrich); NESNO, *Nestor notabilis* (kea); PELSI, *P. sinensis* (Chinese softshell turtle); ANOCA, *Anolis carolinensis* (green anole); ALLMI, *A. mississippiensis* (American alligator); XENTR, *X. tropicallis* (clawed frog); XIPMA, *Xiphophorus maculatus* (platy); TAKRU, *Takifugu rubripes* (pufferfish); PUNNE, *Pundamilia nyererei* (flame black cichlid); ESOLU, *Esox lucius* (Northern pike); ASTME, *Astyanax mexicanus* (Mexican tetra); MAYZE, *Maylandia zebra* (Zebra mbuna); DANRE, *D. rerio* (zebrafish); STEPA, *Stegastes partitus* (bicolor damselfish); ORENI, *Oreochromis niloticus* (Nile tilapia); CALMI, *Callorhynchus milii* (Australian ghost shark); LATCH, *L. chalumnae* (West Indian ocean coelacanth).

unit l, a homologue of subunit k (54), that are unrelated in sequence to any of the bovine subunits and are not encoded in metazoan genomes. Again, each of subunits j, k, and l has a single predicted transmembrane α -helical span.

The present studies have revealed a network of cross-links between exposed lysine residues in the N- and C-terminal regions of bovine subunits e, f, g, DAPIT, and 6.8PL (see Fig. 4). Residue Lys-49 in the C-terminal region of 6.8PL is linked to the C-terminal regions subunits DAPIT, e, and f via cross-links to residues Lys-55, Lys-54, and Lys-79, respectively, and the C-terminal regions of subunits e and f are linked via a cross-link from

Lys-47 in subunit e to Lys-85 in subunit f. Finally, the N-terminal regions of subunit f and g are cross-linked from Lys-15 in subunit f to Lys-65 in subunit g. This network of cross-links shows that the N-terminal regions of all five proteins are on the same side of the lipid bilayer in the intact F-ATPase and that, conversely, all of their C-terminal regions are located on the opposite side of the membrane. Although there is as yet no direct information about the orientations of the subunits in the bovine inner mitochondrial membrane, it is reasonable to assume that subunits e, f, and g have the same orientations as their yeast orthologs. In view of the cross-links between the

C-terminal regions of the 6.8PL, DAPIT, and e subunits, it seems likely that 6.8PL and DAPIT also will be oriented in a similar fashion, as depicted in Fig. 4.

These studies on the supernumerary subunits of the bovine F-ATPase have little or no apparent relevance to the interpretation of the structure of the dimeric F-ATPase from the mitochondria of the alga *Polytomella* sp. at 6.5 Å resolution (55). It is known that the F-ATPase from this species and from the related alga *Chlamydomonas reinhardtii* contains the catalytic core subunits α , β , γ , δ , ϵ , oscp, a, and c plus nine “atypical” subunits (56). Atypical subunits Asa2, Asa4, and Asa7 are thought to be components of the peripheral stalk (57), which is much stouter and more elaborate than the peripheral stalk in the bovine and fungal F-ATPases. The stoichiometry of none of the atypical algal subunits is known, and there is no evident sequence relationship to any of the much more extensively studied peripheral stalk subunits in the bovine enzyme especially (6–10), and there is no relationship either of atypical subunits with any of the supernumerary subunits described here, including ATP8. Indeed, it is not clear whether or not the algal enzymes contain an ATP8 subunit (58). The information in this paper is much more likely to be helpful in establishing relatively high resolution structures of the bovine and fungal enzymes.

References

- Walker, J. E. (2013) The ATP synthase: the understood, the uncertain, and the unknown. *Biochem. Soc. Trans.* **41**, 1–16
- Walker, J. E., Lutter, R., Dupuis, A., and Runswick, M. J. (1991) Identification of the subunits of F_1F_0 -ATPase from bovine heart mitochondria. *Biochemistry* **30**, 5369–5378
- Abrahams, J. P., Leslie, A. G. W., Lutter, R., and Walker, J. E. (1994) Structure at 2.8 Å resolution of F_1 -ATPase from bovine heart mitochondria. *Nature* **370**, 621–628
- Watt, I. N., Montgomery, M. G., Runswick, M. J., Leslie, A. G. W., and Walker, J. E. (2010) Bioenergetic cost of making an adenosine triphosphate molecule in animal mitochondria. *Proc. Natl. Acad. Sci. U.S.A.* **107**, 16823–16827
- Cherepanov, D. A., Mulkidjanian, A. Y., and Junge, W. (1999) Transient accumulation of elastic energy in proton translocating ATP synthase. *FEBS Lett.* **449**, 1–6
- Collinson, I. R., van Raaij, M. J., Runswick, M. J., Fearnley, I. M., Skehel, J. M., Orriss, G. L., Miroux, B., and Walker, J. E. (1994) ATP synthase from bovine heart mitochondria: *in vitro* assembly of a stalk complex in the presence of F_1 -ATPase and in its absence. *J. Mol. Biol.* **242**, 408–421
- Rees, D. M., Leslie, A. G. W., and Walker, J. E. (2009) The structure of the membrane extrinsic region of bovine ATP synthase. *Proc. Natl. Acad. Sci. U.S.A.* **106**, 21597–21601
- Dickson, V. K., Silvester, J. A., Fearnley, I. M., Leslie, A. G. W., and Walker, J. E. (2006) On the structure of the stator of the mitochondrial ATP synthase. *EMBO J.* **25**, 2911–2918
- Walker, J. E., and Dickson, V. K. (2006) The peripheral stalk of the mitochondrial ATP synthase. *Biochim. Biophys. Acta* **1757**, 286–296
- Carbajo, R. J., Kellas, F. A., Yang, J.-C., Runswick, M. J., Montgomery, M. G., Walker, J. E., and Neuhaus, D. (2007) How the N-terminal domain of the OSCP subunit of bovine F_1F_0 -ATP synthase interacts with the N-terminal region of an α subunit. *J. Mol. Biol.* **368**, 310–318
- Baker, L. A., Watt, I. N., Runswick, M. J., Walker, J. E., and Rubinstein, J. L. (2012) Arrangement of subunits in intact mammalian mitochondrial ATP synthase determined by cryo-EM. *Proc. Natl. Acad. Sci. U.S.A.* **109**, 11675–11680
- Fearnley, I. M., and Walker, J. E. (1986) Two overlapping genes in bovine mitochondrial DNA encode membrane components of ATP synthase. *EMBO J.* **5**, 2003–2008
- Collinson, I. R., Runswick, M. J., Buchanan, S. K., Fearnley, I. M., Skehel, J. M., van Raaij, M. J., Griffiths, D. E., and Walker, J. E. (1994) F_0 membrane domain of ATP synthase from bovine heart mitochondria: purification, subunit composition, and reconstitution with F_1 -ATPase. *Biochemistry* **33**, 7971–7978
- Chen, R., Runswick, M. J., Carroll, J., Fearnley, I. M., and Walker, J. E. (2007) Association of two proteolipids of unknown function with ATP synthase from bovine heart mitochondria. *FEBS Lett.* **581**, 3145–3148
- Arnold, I., Pfeiffer, K., Neupert, W., Stuart, R. A., and Schagger, H. (1998) Yeast mitochondrial F_1F_0 -ATP synthase exists as a dimer: identification of three dimer-specific subunits. *EMBO J.* **17**, 7170–7178
- Paumard, P., Vaillier, J., Coulary, B., Schaeffer, J., Soubannier, V., Mueller, D. M., Brèthes, D., di Rago, J. P., and Velours, J. (2002) The ATP synthase is involved in generating mitochondrial cristae morphology. *EMBO J.* **21**, 221–230
- Smith, P. K., Krohn, R. I., Hermanson, G. T., Mallia, A. K., Gartner, F. H., Provenzano, M. D., Fujimoto, E. K., Goeke, N. M., Olson, B. J., and Klenk, D. C. (1985) Measurement of protein using bicinchoninic acid. *Anal. Biochem.* **150**, 76–85
- Laemmli, U. K. (1970) Cleavage of structural proteins during the assembly of the head of bacteriophage T4. *Nature* **227**, 680–685
- Schagger, H., and von Jagow, G. (1991) Blue native electrophoresis for isolation of membrane protein complexes in enzymatically active form. *Anal. Biochem.* **199**, 223–231
- Pullman, M. E., and Monroy, G. C. (1963) A soluble heat stable protein in mitochondria from bovine heart that inhibits ATP hydrolase activity. *J. Biol. Chem.* **238**, 3762–3769
- Runswick, M. J., Bason, J. V., Montgomery, M. G., Robinson, G. C., Fearnley, I. M., and Walker, J. E. (2013) The affinity purification and characterization of ATP synthase complexes from mitochondria. *Open Biol.* **3**, 120160
- Rinner, O., Seebacher, J., Walzthoeni, T., Mueller, L. N., Beck, M., Schmidt, A., Mueller, M., and Aebersold, R. (2008) Identification of cross-linked peptides from large sequence databases. *Nat. Methods* **5**, 315–318
- Seebacher, J., Mallick, P., Zhang, N., Eddes, J. S., Aebersold, R., and Gelb, M. H. (2006) Protein cross-linking analysis using mass spectrometry, isotope-coded cross-linkers, and integrated computational data processing. *J. Proteome Res.* **5**, 2270–2282
- Shevchenko, A., Tomas, H., Havlis, J., Olsen, J. V., and Mann, M. (2006) In-gel digestion for mass spectrometric characterization of proteins and proteomes. *Nat. Protoc.* **1**, 2856–2860
- Perkins, D. N., Pappin, D. J., Creasy, D. M., and Cottrell, J. S. (1999) Probability-based protein identification by searching sequence databases using mass spectrometry data. *Electrophoresis* **20**, 3551–3567
- Holding, A. N., Lamers, M. H., Stephens, E., and Skehel, J. M. (2013) Hekate: software suite for the mass spectrometric analysis and three-dimensional visualization of cross-linked protein samples. *J. Proteome Res.* **12**, 5923–5933
- Cox, J., Neuhauser, N., Michalski, A., Scheltema, R. A., Olsen, J. V., and Mann, M. (2011) Andromeda: a peptide search engine integrated into the MaxQuant environment. *J. Proteome Res.* **10**, 1794–1805
- DeLano, W. L. (2010) *The PyMOL Molecular Graphics System*, Version 1.5, Schrodinger, LLC, New York
- Emsley, P., Lohkamp, B., Scott, W. G., and Cowtan, K. (2010) Features and development of Coot. *Acta Crystallogr. D Biol. Crystallogr.* **66**, 486–501
- Larkin, M. A., Blackshields, G., Brown, N. P., Chenna, R., McGettigan, P. A., McWilliam, H., Valentin, F., Wallace, I. M., Wilm, A., Lopez, R., Thompson, J. D., Gibson, T. J., and Higgins, D. G. (2007) ClustalW and ClustalX version 2.0. *Bioinformatics* **23**, 2947–2948
- Tusnady, G. E., and Simon, I. (2001) The HMMTOP transmembrane topology prediction server. *Bioinformatics* **17**, 849–850
- Buchan, D. W., Minneci, F., Nugent, T. C., Bryson, K., and Jones, D. T. (2013) Scalable web services for the PSIPRED Protein Analysis Workbench. *Nucleic Acids Res.* **41**, W349–W357
- Macreadie, I. G., Novitski, C. E., Maxwell, R. J., John, U., Ooi, B. G., McMullen, G. L., Lukins, H. B., Linnane, A. W., and Nagley, P. (1983) Biogenesis of mitochondria: the mitochondrial gene (aap1) coding for mitochondrial ATPase subunit 8 in *Saccharomyces cerevisiae*. *Nucleic Acids Res.* **11**, 4435–4451

Membrane Subunits of Bovine F-ATPase

34. Velours, J., Esparza, M., Hoppe, J., Sebald, W., and Guerin, B. (1984) Amino acid sequence of a new mitochondrially synthesized proteolipid of the ATP synthase of *Saccharomyces cerevisiae*. *EMBO J.* **3**, 207–212
35. Gissi, C., Iannelli, F., and Pesole, G. (2008) Evolution of the mitochondrial genome of Metazoa as exemplified by comparison of congeneric species. *Heredity* **101**, 301–320
36. Anderson, S., Bankier, A. T., Barrell, B. G., de Bruijn, M. H. L., Coulson, A. R., Drouin, J., Eperon, I. C., Nierlich, D. P., Roe, B. A., Sanger, F., Schreier, P. H., Smith, A. J., Staden, R., and Young, I. G. (1981) Sequence and organization of the human mitochondrial genome. *Nature* **290**, 457–465
37. Stephens, A. N., Khan, M. A., Roucou, X., Nagley, P., and Devenish, R. J. (2003) The molecular neighborhood of subunit 8 of yeast mitochondrial F₁F₀-ATP synthase probed by cysteine scanning mutagenesis and chemical modification. *J. Biol. Chem.* **278**, 17867–17875
38. Collinson, I. R., Fearnley, I. M., Skehel, J. M., Runswick, M. J., and Walker, J. E. (1994) ATP synthase from bovine heart mitochondria: identification by proteolysis of sites in F₀ exposed by removal of F₁ and the oligomycin-sensitivity conferral protein. *Biochem. J.* **303**, 639–645
39. Belogrudov, G. I., Tomich, J. M., and Hatefi, Y. (1996) Membrane topography and near-neighbor relationships of the mitochondrial ATP synthase subunits e, f, and g. *J. Biol. Chem.* **271**, 20340–20345
40. Stephens, A. N., Roucou, X., Artika, I. M., Devenish, R. J., and Nagley, P. (2000) Topology and proximity relationships of yeast mitochondrial ATP synthase subunit 8 determined by unique introduced cysteine residues. *Eur. J. Biochem.* **267**, 6443–6451
41. Jonckheere, A. I., Hogeveen, M., Nijtmans, L. G., van den Brand, M. A., Janssen, A. J., Diepstra, J. H., van den Brandt, F. C., van den Heuvel, L. P., Hol, F. A., Hofste, T. G., Kapusta, L., Dillmann, U., Shamdeen, M. G., Smeitink, J. A., and Rodenburg, R. J. (2008) A novel mitochondrial ATP8 gene mutation in a patient with apical hypertrophic cardiomyopathy and neuropathy. *J. Med. Genet.* **45**, 129–133
42. Nagley, P., Farrell, L. B., Gearing, D. P., Nero, D., Meltzer, S., and Devenish, R. J. (1988) Assembly of functional proton-translocating ATPase complex in yeast mitochondria with cytoplasmically synthesized subunit 8, a polypeptide normally encoded within the organelle. *Proc. Natl. Acad. Sci. U.S.A.* **85**, 2091–2095
43. Grasso, D. G., Nero, D., Law, R. H., Devenish, R. J., and Nagley, P. (1991) The C-terminal positively charged region of subunit 8 of yeast mitochondrial ATP synthase is required for efficient assembly of this subunit into the membrane F₀ sector. *Eur. J. Biochem.* **199**, 203–209
44. Spannagel, C., Vaillier, J., Arselin, G., Graves, P. V., and Velours, J. (1997) The subunit f of mitochondrial yeast ATP synthase: characterization of the protein and disruption of the structural gene ATP17. *Eur. J. Biochem.* **247**, 1111–1117
45. Arselin, G., Giraud, M. F., Dautant, A., Vaillier, J., Brèthes, D., Couлары-Salin, B., Schaeffer, J., and Velours, J. (2003) The GXXXG motif of the transmembrane domain of subunit e is involved in the dimerization/oligomerization of the yeast ATP synthase complex in the mitochondrial membrane. *Eur. J. Biochem.* **270**, 1875–1884
46. Bustos, D. M., and Velours, J. (2005) The modification of the conserved GXXXG motif of the membrane-spanning segment of subunit g destabilizes the supramolecular species of yeast ATP synthase. *J. Biol. Chem.* **280**, 29004–29010
47. Velours, J., Spannagel, C., Chaignepain, S., Vaillier, J., Arselin, G., Graves, P. V., Velours, G., and Camougrand, N. (1998) Topography of the yeast ATP synthase F₀ sector. *Biochimie* **80**, 793–801
48. Arselin, G., Vaillier, J., Salin, B., Schaeffer, J., Giraud, M.-F., Dautant, A., Brèthes, D., and Velours, J. (2004) The modulation in subunits e and g amounts of yeast ATP synthase modifies mitochondrial cristae morphology. *J. Biol. Chem.* **279**, 40392–40399
49. Roudeau, S., Spannagel, C., Vaillier, J., Arselin, G., Graves, P. V., and Velours, J. (1999) Subunit f of the yeast mitochondrial ATP synthase: topological and functional studies. *J. Bioenerg. Biomembr.* **31**, 85–94
50. Meyer, B., Wittig, I., Trifilieff, E., Karas, M., and Schägger, H. (2007) Identification of two proteins associated with mammalian ATP synthase. *Mol. Cell Proteomics* **6**, 1690–1699
51. Ohsakaya, S., Fujikawa, M., Hisabori, T., and Yoshida, M. (2011) Knockdown of DAPIT (diabetes-associated protein in insulin-sensitive tissue) results in loss of ATP synthase in mitochondria. *J. Biol. Chem.* **286**, 20292–20296
52. Vaillier, J., Arselin, G., Graves, P. V., Camougrand, N., and Velours, J. (1999) Isolation of supernumerary yeast ATP synthase subunits e and i. Characterization of subunit i and disruption of its structural gene ATP18. *J. Biol. Chem.* **274**, 543–548
53. Arnold, I., Pfeiffer, K., Neupert, W., Stuart, R. A., and Schägger, H. (1999) ATP synthase of yeast mitochondria—Isolation of subunit j and disruption of the ATP18 gene. *J. Biol. Chem.* **274**, 36–40
54. Liu, S., Charlesworth, T. J., Bason, J. V., Montgomery, M. G., Harbour, M. E., Fearnley, I. M., and Walker, J. E. (2015) The purification and characterization of ATP synthase complexes from the mitochondria of four fungal species. *Biochem. J.* 10.1042/BJ20150197
55. Allegretti, M., Klusch, N., Mills, D. J., Vonck J., Kühlbrandt, W., and Davies, K. M. (2015) Horizontal membrane-intrinsic α -helices in the stator a-subunit of an F type ATP synthase. *Nature* 10.1038/nature14185
56. Vázquez-Acevedo, M., Cardol, P., Cano-Estrada, A., Lapaille, M., Remacle, C., González-Halphen, D., (2006) The mitochondrial ATP synthase of chlorophycean algae contains eight subunits of unknown origin involved in the formation of an atypical stator-stalk and in the dimerization of the complex. *J. Bioenerg. Biomembr.* **38**, 271–282
57. Miranda-Astudillo, H., Cano-Estrada, A., Vázquez-Acevedo, M., Colina-Tenorio, L., Downie-Velasco, A., Cardol, P., Remacle, C., Domínguez-Ramírez, L., González-Halphen, D. (2014) Interactions of subunits Asa2, Asa4, and Asa7 in the peripheral stalk of the mitochondrial ATP synthase of the chlorophycean alga *Polytomella* sp. *Biochim. Biophys. Acta* **1837**, 1–13
58. van Lis, R., Mendoza-Hernández, G., Groth, G., and Atteia, A. (2007) New insights into the unique structure of the F₀F₁-ATP synthase from the chlamydomonad algae *Polytomella* sp. and *Chlamydomonas reinhardtii*. *Plant Physiol.* **144**, 1190–1199